

ISL1 and BRN3B co-regulate the differentiation of murine retinal ganglion cells

Ling Pan¹, Min Deng¹, Xiaoling Xie¹ and Lin Gan^{1,2,3,*}

LIM-homeodomain (HD) and POU-HD transcription factors play crucial roles in neurogenesis. However, it remains largely unknown how they cooperate in this process and what downstream target genes they regulate. Here, we show that ISL1, a LIM-HD protein, is co-expressed with BRN3B, a POU-HD factor, in nascent post-mitotic retinal ganglion cells (RGCs). Similar to the *Brn3b*-null retinas, retina-specific deletion of *Isl1* results in the apoptosis of a majority of RGCs and in RGC axon guidance defects. The *Isl1* and *Brn3b* double null mice display more severe retinal abnormalities with a near complete loss of RGCs, indicating the synergistic functions of these two factors. Furthermore, we show that both *Isl1* and *Brn3b* function downstream of *Math5* to regulate the expression of a common set of RGC-specific genes. Whole-retina chromatin immunoprecipitation and in vitro transactivation assays reveal that ISL1 and BRN3B concurrently bind to and synergistically regulate the expression of a common set of RGC-specific genes. Thus, our results uncover a novel regulatory mechanism of BRN3B and ISL1 in RGC differentiation.

KEY WORDS: LIM-homeodomain, POU domain, MATH5, ATOH7, POU4F2, RGC, Retinal development, Transcription factor

INTRODUCTION

Owing to its easy accessibility and well-organized laminar structure, the retina has long served as an ideal experimental model for studying the central nervous system (CNS). Retinogenesis in vertebrates is stereotyped in an ordered fashion: retinal ganglion cells (RGCs) are always born first; immediately followed by horizontal, amacrine and cone cells; and last by bipolar, rod and Müller cells (Cepko et al., 1996; Young, 1985). During RGC development, the basic helix-loop-helix (bHLH) transcription factor (TF), MATH5 (ATOH7 – Mouse Genome Informatics), is expressed in post-mitotic retinal precursors and provides them with the competency to become RGCs (Yang et al., 2003). MATH5 regulates the expression of RGC-specific differentiating TFs such as the POU-homeodomain (POU-HD) factor BRN3B (POU4F2 – Mouse Genome Informatics) and the LIM-homeodomain (LIM-HD) factor ISL1 (Wang et al., 2001; Yang et al., 2003). In *Math5*-deficient mice, fewer than 5% of RGCs are generated (Brown et al., 2001; Wang et al., 2001). In contrast to the early function of MATH5 in RGC genesis, BRN3B expression starts in nascent RGCs and is required for their terminal differentiation, including axon outgrowth and pathfinding, and for cell survival (Erkman et al., 2000; Gan et al., 1999; Pan et al., 2005; Xiang, 1998). In *Brn3b*-null mice, RGCs are initially generated but 80% of them undergo apoptosis before birth (Erkman et al., 1996; Gan et al., 1996). Moreover, the compound mutation of *Brn3b* and *Brn3c* (*Pou4f3* – Mouse Genome Informatics) results in the further reduction of RGCs in adult mice (Wang et al., 2002a). Although previous studies have shown clearly the importance of BRN3 factors in RGC development, it remains poorly understood how RGC differentiation is regulated and whether other TFs control this process in parallel to BRN3 factors.

Studies of CNS development in both vertebrates and invertebrates have shown that TFs, often acting in distinct combinatorial manner, play important roles during neurogenesis (Bang and Goulding, 1996; Castro et al., 2006; Lee and Pfaff, 2001). The POU-HD and LIM-HD TFs appear to function primarily at the later stages of neurogenesis. For example, in the spinal cord, the unique combinatorial expression of LIM-HD TFs confers motoneuron subtypes with specific axon targeting pathways (Appel et al., 1995; Kania et al., 2000; Sharma et al., 2000; Sharma et al., 1998; Tsuchida et al., 1994). BRN3B is required in the development of RGCs (discussed above). In *Drosophila*, Acj6 and Drifter (Vvl – FlyBase), both POU-HD TFs, are required for the dendritic targeting in olfactory system (Komiya et al., 2003). Moreover, LIM-HD and POU-HD TFs have been shown to cooperate in regulating neuronal differentiation. One such example is the regulation of touch receptor differentiation in *C. elegans* by POU-HD factor UNC-86 and LIM-HD factor MEC-3. UNC-86 dimerizes with MEC-3 on the *mec-3* promoter, which is required for the maintenance of *mec-3* expression and touch cell differentiation (Lichtsteiner and Tjian, 1995; Xue et al., 1993). UNC-86 and MEC-3 also synergistically activate the touch cell-specific genes *mec-4* and *mec-7* (Duggan et al., 1998).

ISL1, one of the founding members of LIM-HD TFs in the Islet subgroup, has been intensively studied in the spinal cord. ISL1 is expressed in all motoneurons immediately after they exit cell cycle and is essential for the genesis of motoneurons (Pfaff et al., 1996). By contrast, *Drosophila* Islet is not required for the genesis of motoneurons, but for the axonal trajectory selection and neurotransmitter expression (Thor and Thomas, 1997). Here, we demonstrate the co-expression of BRN3B and ISL1 in post-mitotic, differentiating RGCs. To investigate the role of ISL1 in RGC development, we generate *Isl1-lacZ* knock-in and *Isl1* conditional knockout mice. We demonstrate that in *Isl1*-null retinas, RGCs appear to be generated normally but 67% RGCs subsequently undergo apoptosis and RGC axon growth is defective, a phenotype strongly resembling that of *Brn3b* mutants (Erkman et al., 2000; Gan et al., 1999). In *Isl1* and *Brn3b* double null retinas, greater than 95% nascent RGCs die of apoptosis, suggesting their cooperative relationship in RGC development. Furthermore, chromatin immunoprecipitation (ChIP) and in vitro transactivation assays

¹Department of Ophthalmology, University of Rochester, Rochester, NY 14642, USA.

²Center for Neural Development and Disease, University of Rochester, Rochester, NY 14642, USA. ³Department of Neurobiology and Anatomy, University of Rochester, Rochester, NY 14642, USA.

* Author for correspondence (e-mail: lin_gan@urmc.rochester.edu)

demonstrate that both factors bind to and regulate the expression of RGC-specific genes. Our data strongly argue for the involvement of both parallel and cooperative functions of ISL1 and BRN3B in RGC development.

MATERIALS AND METHODS

Animals

Brn3b^{lacZ}, *Brn3b^{AP}* and *Six3-cre* mice have been previously described (Furuta et al., 2000; Gan et al., 1999). *Isl2^{lacZ}* knock-in mice (L. Gan, unpublished) were generated by replacing all the *Isl2*-coding sequences with a *lacZ-SV40 polyA-Neo* cassette. The *Isl1^{lacZ}* targeting construct was generated by inserting the *Isl1* 2.6 kb 5'- and 4.2 kb 3'-flanking sequences into the 5' and 3' multiple cloning sites of PKII-lacZ vector (L. Gan, unpublished), where a cassette with *lacZ-SV40 polyA-Neo* replaced *Isl1* exon 1-2 and adjacent intron sequences. To make the *Isl1^{CKO}* targeting construct, we inserted a neomycin resistance gene along with a loxP site at the 5' of exon 2, and another loxP site at the 3' of exon 2. The targeting vectors were electroporated into W4 mouse embryonic stem cells (Auerbach et al., 2000) to generate *Isl1^{lacZ/+}* and *Isl1^{CKO/+}* mice. *Isl1^{loxP/+}* mice were obtained by crossing *Isl1^{CKO/+}* mice with the ROSA26-FLPe mice (The Jackson Laboratory, Stock Number: 003946) to remove FRT-flanked neomycin resistance gene.

The PCR genotyping of these animals was performed as follows: 5'-AGGGCCGCAAGAAAACATATCC and 5'-ACTTCGGCACCTTACGCTTCTTCT to detect a 404 bp product of *Isl1^{lacZ}* allele; 5'-GGT-GCTTAGCGGTGATTCTCTC and 5'-GCACTTTGGGATGGTAATTGGAG to detect a 452 bp product of WT *Isl1* allele and a 512 bp product of *Isl1^{loxP}* allele; and 5'-GTGGAATCGCTGAATCTTGAC and 5'-GCCCAAATGTTGCTGGATAGT to detect *Six3-cre* allele. The mouse strains were maintained in the C57BL/6J and 129S6 mixed background. Embryonic day 0.5 (E0.5) was defined as the day when the vaginal plug appeared. University Committee of Animal Resources at the University of Rochester approved all animal procedures.

Hematoxylin and Eosin (H&E) staining, immunohistochemistry, X-Gal staining and in situ hybridization

Embryos were harvested from E11.5 to E18.5, decapitated and fixed in 4% paraformaldehyde in phosphate-buffered saline (PBS) for several hours and were processed for paraffin sections or cryosections. Horizontal retina sections across optic disc collected from controls and mutant littermates were mounted side by side for comparisons. BrdU labeling, H&E and X-Gal staining were carried out as previously reported (Pan et al., 2005). The primary antibodies used in immunohistochemistry were: mouse anti-BRN3A (POU4F1 – Mouse Genome Informatics) (Santa Cruz, 1:200), goat anti-BRN3B (Santa Cruz, 1:200), mouse anti-ISL1 (Developmental Studies Hybridoma Bank, 1:200), mouse anti-bromodeoxyuridine (BrdU) (Becton Dickinson, 1:400), rabbit anti-phosphorylated histone 3 (Santa Cruz, 1:400), mouse anti-SMI32 (Sternberger Monoclonals, 1:1000) and rabbit anti-activated caspase 3 (R&D Systems, 1:100). The Alexa-conjugated secondary antibodies (Molecular Probes) were used at 1:1000 dilution. Non-radioactive in situ hybridization was performed using digoxigenin-UTP labeled riboprobes (Radde-Gallwitz et al., 2004). The specific cDNA sequences used to generate riboprobes were: *Brn3a* (3' UTR); *Olf1* (L12147, nucleotides 865-1180); *Irx4* (NM_018885, nucleotides 1556-2265); *Ablim1* (AF316037, nucleotides 12-31); *L1cam* (NM_008478, nucleotides 3083-3748). *Isl1* and *Isl2* probes were described previously (Yang et al., 2003). The *Shh* probe was a generous gift from Dr Valerie A. Wallace (Jensen and Wallace, 1997). Confocal images were acquired on an Olympus microscope (BX50WI) with Fluoview 4.3 laser scanning. Other pictures were taken with a Nikon Eclipse TE2000-U inverted microscope with a Nikon DXM1200F digital camera.

Cell counts and statistical analysis

For apoptosis analysis, five pairs of matched retina sections of *Isl1*-null and littermate controls were collected at regularly spaced intervals to completely survey each retina. After anti-activated caspase 3 immunolabeling, images were taken and the immunoreactive cells were counted with Image J program (NIH). Results from five sections were averaged to obtain the

apoptotic cell number for each eye. For analyses of BRN3A+ or BRN3B+ cells, whole-mount retinas were used. In these cases, three pictures were obtained from the central region of the retinas. The immunoreactive cells were counted and averaged. To compare the optic nerve size, three pairs of matched cross-sections of null and control optic nerves were collected and processed for H&E staining. The boundary of each optic nerve was outlined using Adobe Photoshop. The size of optic nerve was determined by measuring the number of pixels contained in the outlined area.

Lipophilic dye tracing

For anterograde labeling of the optic pathway, mouse heads at E13.5 and E15.5 were fixed overnight in 4% paraformaldehyde in PBS. After enucleation of the right eye, DiI crystals (Molecular Probes) were implanted unilaterally in the optic disc. After incubation in PBS containing 0.1% sodium azide at 37°C for 1-2 weeks, the brains were dissected to expose the optic chiasm and visualized under a Nikon SMZ1500 fluorescent stereomicroscope.

Chromatin immunoprecipitation (ChIP)

Chromatin from retinas at indicated stages was collected according to the protocol supplied with the ChIP assay kit (Upstate Biotechnologies). Mouse anti-ISL1 and goat anti-BRN3B were used for immunoprecipitation. Promoter regions with BRN3-binding consensus sequences were detected in the precipitated material by PCR (primer set details can be provided on request). *Brn3b* ORF was used as a negative control.

Luciferase activity assay

CV1 epithelial cells were cultured in 24-well plates in DMEM with 10% FBS. Transfections were carried out with Lipofectamine 2000 (Invitrogen) when cells reached 70% confluence. *Brn3b* expression plasmid and *Brn3a*-luciferase reporter construct were generous gifts from Dr Eric Turner (Trieu et al., 2003). *Isl1* expression plasmid was generated by inserting *Isl1* cDNA into pCDNA expression vector (Invitrogen). For each transfection, 100 ng of *Isl1* and/or *Brn3b* expression plasmid, 200 ng of *Brn3a*-luciferase reporter construct and 5 ng of *PRL* (Promega) *Renilla* luciferase control plasmid were used. The total amount of DNA was balanced by adding empty pCDNA vector. Cells were harvested 36 hours after transfection and luciferase activity was measured with the Dual-Luciferase Reporter Assay System (Promega). The firefly luciferase activity was normalized by renilla luciferase activity.

RESULTS

Co-localization of ISL1 and BRN3B in post-mitotic RGCs

To address the functions of ISL1 in RGC differentiation, we first compared its spatiotemporal expression pattern in developing retinas with that of BRN3B, one of the earliest RGC markers. At E11.5, nascent RGCs were first found in the central retina and co-expressed ISL1 and BRN3B (Fig. 1A-C, arrows). At E13.5, as retinogenesis proceeded in a central-to-peripheral wave, more RGCs were co-labeled with ISL1 and BRN3B (Fig. 1D-F). Although the overall expression pattern was almost identical for these two factors, there was a slight difference in the signal intensity in the labeled cells. Whereas BRN3B was expressed uniformly in both migrating RGCs in the neuroblast layer (NBL) and the post-migrated RGCs in the ganglion cell layer (GCL), ISL1 expression level appeared to be higher in the GCL and lower in the NBL. The expression of ISL1 was sustained in RGCs in adult mice and was also found in cholinergic amacrine and ON-bipolar cells (Elshatory et al., 2007a; Elshatory et al., 2007b; Galli-Resta et al., 1997). Anti-ISL1 is raised against the C-terminal of ISL1 homeodomain and reacts to ISL1 specifically but also recognizes ISL2 with a lower affinity (Tanabe et al., 1998). In mouse, weak ISL2 expression is first detected in a very few RGCs in the central GCL at E13.5 and in about 30% RGCs postnatally (see Fig. S1A-D in the supplementary material) (Brown et al., 2000; Pak et al., 2004). Targeted deletion of *Isl2* reveals that

Isl2 is not necessary for the generation and survival of RGCs (Pak et al., 2004). To confirm that the above anti-ISL1 labeling reveals the true *Isl1* expression pattern, we compared the ISL1-immunostaining in wild-type (WT) and *Isl2*-null retinas at E13.5 to E15.5 and found no difference in the labeling patterns (Fig. 1D-F, data not shown; see Fig. S1E-J in the supplementary material). Thus, at E11.5 to E15.5, all cells labeled with anti-ISL1 in the retina represent ISL1-expressing cells.

The detection of ISL1 in the NBL suggested that it is expressed in retinal progenitors. To test this possibility, we performed immunostaining with anti-ISL1 in conjunction with several cell

cycle markers, BrdU labeling to mark S-phase cells and anti-phosphorylated histone 3 (pH3) staining to identify M-phase cells. At E12.5, when both proliferating progenitors and post-mitotic RGCs were readily detectable, ISL1 expression was detected mostly in cells negative for BrdU and pH3 (Fig. 1G-L). Thus, ISL1 is predominantly expressed in post-mitotic cells during early retinogenesis.

The early expression of ISL1 in nascent RGCs and its colocalization with BRN3B suggested that ISL1 could function in parallel to BRN3B or immediately upstream or downstream of BRN3B during RGC development. To distinguish these possibilities, we analyzed the expression of ISL1 in *Math5*-null and *Brn3b*-null mice. In *Math5*-null retinas at E13.5, the expression of ISL1 and BRN3B was dramatically decreased (Fig. 1M,N,P,Q), consistent with our previous finding that *Brn3b* and *Isl1* are downstream genes of *Math5* (Wang et al., 2001; Yang et al., 2003). By contrast, we observed no discernible changes in *Isl1* expression in *Brn3b*-null retinas at E14.5 (Fig. 1O,R), a stage before the onset of RGC death caused by the absence of *Brn3b* (Gan et al., 1999). Therefore, *Isl1* probably functions upstream of or in parallel to *Brn3b* during RGC development.

Targeted disruption of *Isl1* in retina

Conventional *Isl1* knockout mice do not survive beyond E11.5, probably owing to the failure in vascular development (Pfaff et al., 1996). To assess the role of ISL1 in RGC development that occurs during mid- to late gestation stages, we generated an *Isl1* conditional knockout allele (*Isl1*^{loxP}) by flanking exon 2, which encodes the first LIM domain, with loxP sequences (Fig. 2A). Cre recombinase-mediated deletion of the loxP-flanked exon 2 resulted in a null mutation via a reading frame shift. Additionally, a *lacZ* knock-in allele, *Isl1*^{lacZ}, was created by replacing the exon 2 with a nuclear *lacZ* reporter gene (Fig. 2B). The genotypes of *Isl1* mutant mice were confirmed by Southern blotting and PCR (Fig. 2C). The expression of β -galactosidase in *Isl1*^{lacZ/+} mice faithfully recapitulated the pattern of endogenous *Isl1* as shown by in situ hybridization and immunostaining (see Fig. S2 in the supplementary material) and, thus, served as an excellent marker of *Isl1*-expressing cells.

Retina-specific removal of *Isl1* was achieved by breeding heterozygous *Isl1*^{lacZ/+} or *Isl1*^{loxP/+} with *Six3-cre* mice and subsequently crossing with *Isl1*^{loxP/loxP} mice. *Six3-cre* mice express Cre recombinase in the eye field and the ventral forebrain from E9 to E9.5 (Furuta et al., 2000), and have been used successfully as an effective retina-specific deleter (Mu et al., 2005b). In our experiments, we observed consistently a greater than 90% deletion of *Isl1* in *Isl1*^{loxP/lacZ}; *Six3-cre* and *Isl1*^{loxP/loxP}; *Six3-cre* retinas at E13.5 (Fig. 2D; data not shown). In the following experiments, *Isl1*^{loxP/lacZ}; *Six3-cre* and *Isl1*^{loxP/loxP}; *Six3-cre* mice were used interchangeably as *Isl1* nulls. *Isl1*^{loxP/+}, *Isl1*^{loxP/loxP} and wild-type mice were phenotypically indistinguishable and were designated as controls hereafter. The *Isl1* nulls were born at Mendelian frequencies (26%, $n=96$) with no overt morphological defects, but exhibited moderate growth retardation postnatally. Their body weights were about 91% of their littermate controls at P10 ($n=7$ pairs) and about 80% at 6 weeks ($n=5$ pairs).

Major loss of RGCs in the absence of *Isl1*

To assess the importance of ISL1 during RGC development, we analyzed BRN3B expression in *Isl1*-null retinas at different embryonic stages (Fig. 3A-H). At E13.5 and E15.5, the peak period of RGC generation, there was no substantial difference in the

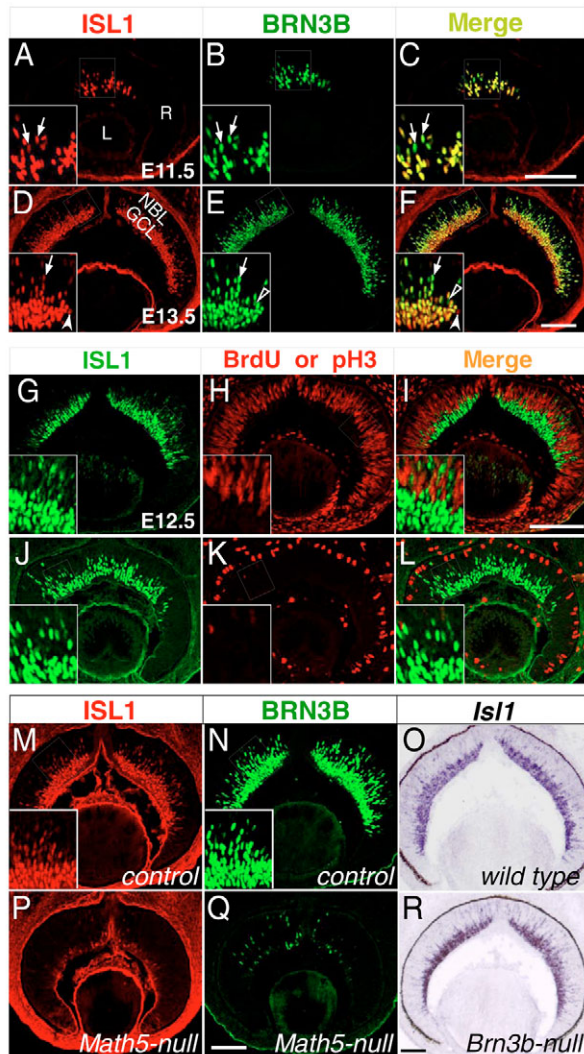


Fig. 1. Expression of ISL1 in developing mouse retina. (A-F) The expression of ISL1 (red) is largely co-localized with that of BRN3B (green) in both migrating RGCs in the NBL and post-migrated RGCs in the GCL (arrows). Open and filled arrowheads indicate the occasional RGCs expressing BRN3B or ISL1 alone, respectively. (G-L) Most of ISL1+ cells (green) are not co-labeled with S- and M-phase markers (red), anti-BrdU (G-I) and anti-pH3 (J-L). (M-R) Expression of *Isl1* is regulated by *Math5* but not by *Brn3b*. (M,N,P,Q) Reduced expression of ISL1 (red) and BRN3B (green) in E13.5 *Math5*-null retinas. (O,R) The comparable *Isl1* expression in wild-type (O) and *Brn3b*-null (R) retinas by in situ hybridization at E14.5. Insets show selected regions at higher magnification. R, retina; L, lens; NBL, neuroblast layer; GCL, ganglion cell layer. Scale bars: 100 μ m.

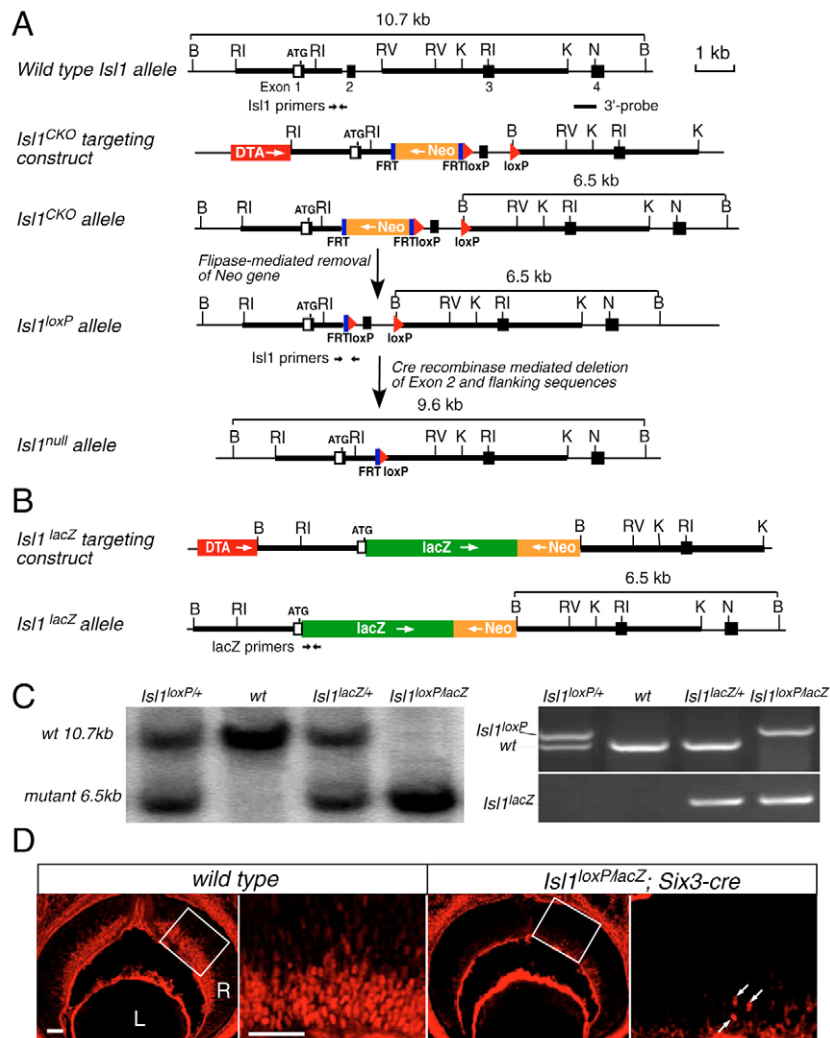


Fig. 2. Generation of *Is11* conditional knockout and *Is11*-*lacZ* knock-in alleles. (A) Generation of *Is11* conditional allele (*Is11*^{CKO}). *Is11* genomic structure and restriction enzyme map is shown at the top. White boxes are the non-coding exon sequences and black boxes the coding sequences. Thick bars are the sequences used to generate the homologous arms in the targeting vector. (B) Generation of *Is11*^{lacZ} knock-in allele. Neo, PGK-neomycin resistance gene; DTA, diphtheria toxin gene for negative selection of embryonic stem cells; *lacZ*, β-galactosidase-encoding gene; FRT, flippase recognition sequence; loxP, Cre recombinase recognition sequence; B, *Bam*HI; RI, *Eco*RI; RV, *Eco*RV; K, *Kpn*I; N, *Not*I. (C) Left panel, Southern genotyping confirmation of *Is11*^{lacZ} and *Is11*^{loxP} mice using 3' probe and *Bam*HI digestion. Right panel, PCR genotyping using primers indicated in A&B can distinguish *Is11*^{loxP}, *Is11*^{lacZ} and wild-type allele. (D) Anti-ISL1 immunolabeling of E13.5 retina sections confirms the deletion of ISL1 in the retina of *Is11*^{loxP}/*Is11*^{lacZ}; *Six3*-Cre mice. The enlarged views of the corresponding boxed regions are shown on the right. Arrows indicate residual ISL1 expression. R, retina; L, lens. Scale bars: 50 μm.

number and distribution of BRN3B⁺ RGCs in *Is11*-null retinas compared with controls (Fig. 3A,B,E,F), indicating that *Is11* is dispensable for the generation and migration of RGCs and for the onset of BRN3B expression. However, BRN3B⁺ RGCs were drastically reduced in the absence of *Is11* at E17.5 (Fig. 3C,G). This reduction progressed in a central-to-peripheral wave and was most evident at E18.5 (Fig. 3D,H).

To determine whether the progressive loss of BRN3B⁺ RGCs resulted from apoptosis, we examined the number of apoptotic cells in control and *Is11*-null retinas. The developmental RGC death normally takes place in the first postnatal week to eliminate false axon connections (Farah and Easter, 2005; Perry et al., 1983). Consistently, we detected few apoptotic cells in wild-type retinas throughout embryogenesis. In *Is11*-null retinas, although there was no significant change in the number of apoptotic cells during the peak of RGC genesis at E13.5 to E15.5, a significant increase in the number of apoptotic cells was detected from E16.5 (2.8-fold of the wild-type level at E16.5, *t*-test *P*<0.01; 5.3-fold at E17.5, *P*<0.01; and 2.6 fold at E18.5, *P*<0.05, Fig. 3K). The apoptotic cells were primarily detected in the GCL (Fig. 3I,J) and the timing of increased apoptosis corresponded to the massive loss of BRN3B⁺ RGCs.

To quantify RGC loss as a result of *Is11*-null mutation, we performed whole-mount immunostaining of adult retinas using anti-BRN3A and BRN3B antibodies (Fig. 4A-E). In adult retinas,

BRN3A and BRN3B are each expressed in ~70% of RGCs in a partially overlapping pattern and their combined expression reveals nearly the entire RGC population (Xiang et al., 1995). In *Is11*-null retinas, both BRN3A⁺ and BRN3B⁺ cells were reduced to about 33% of those in wild type. To rule out the possibility that this reduction was due to the downregulation of BRN3A and BRN3B, rather than the loss of RGCs, we also analyzed RGC axons as another parameter of RGC number. SMI32 antibody recognizes a non-phosphorylated epitope on the neurofilament H-chain and specifically labels large RGCs and their nerve fibers (Nixon et al., 1989). In *Is11*-null retinas, the number of SMI32⁺ axon bundles was significantly reduced and the remaining ones appeared to be less fasciculated (Fig. 4F,G). Consistently, the ventral view of mouse brains revealed that *Is11* nulls have much thinner optic nerves, optic chiasmata and optic tracts (Fig. 4H,I). Quantification analysis showed a 69% reduction in the cross-section area of optic nerves in *Is11* nulls. These data indicate that ISL1 is required for RGC survival but not for the generation and migration of RGCs or for the initiation of BRN3B expression in retinas.

ISL1 and BRN3B regulate common downstream target genes

The co-expression of ISL1 and BRN3B raises the possibility that they regulate a common set of downstream genes in differentiating RGCs. To test this possibility, we examined retinas at E14.5, a time

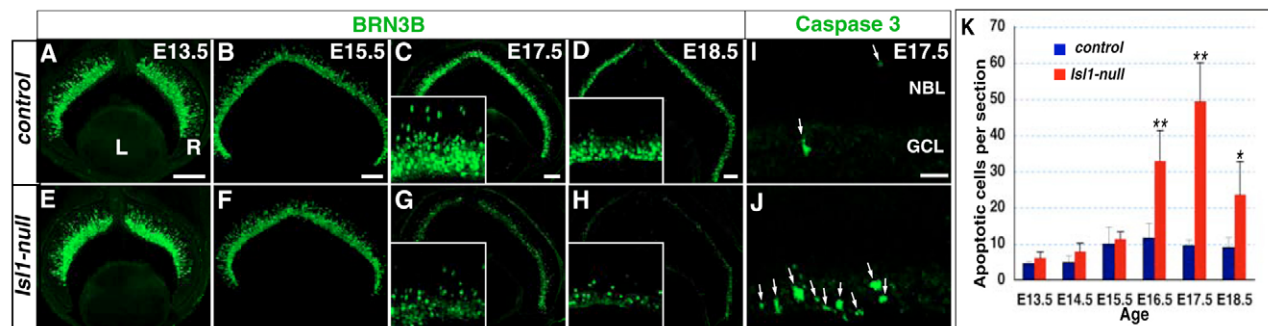


Fig. 3. Targeted disruption of *Isl1* results in the developmental loss of RGCs. (A-H) Immunostaining of retina sections with anti-BRN3B reveals a significant loss of BRN3B+ RGCs in *Isl1* nulls at E17.5 (C,G) and E18.5 (D,H). Insets show the enlarged views of the central retina. (I,J) Anti-activated caspase3 immunostaining shows an increase in apoptotic cells (arrows) in the GCL of *Isl1*-null retina. (K) The difference of apoptotic cell numbers in wild-type and *Isl1*-null retina is insignificant at E13.5-15.5. However, in *Isl1* nulls, the apoptotic cells are significantly increased from E16.5. Each histogram represents the mean+s.d. $n=3$ or 4 for each genotype per stage. * $P<0.05$, ** $P<0.01$; t -test. R, retina; L, lens; NBL, neuroblast layer; GCL, ganglion cell layer. Scale bars: 100 μ m in A-D; 25 μ m in I.

point at which neither the reduction of BRN3B expression nor the progressive RGC apoptosis has occurred. BRN3A, ISL2, IRX4, and OLF1 (EBF1 – Mouse Genome Informatics) are TFs whose expression immediately follows that of BRN3B during retinal development. BRN3A is expressed in the post-migrated RGCs

starting from E12.5 and is thought to play a redundant role with BRN3B (Pan et al., 2005). ISL2 is selectively expressed in one-third of contralaterally projecting RGCs and represses the ipsilateral targeting program (Pak et al., 2004). IRX4 is involved in intra-retina pathfinding of RGCs (Jin et al., 2003). OLF1, with an early onset of retinal expression from E12.5 (Xiang, 1998), has no identified function in RGC differentiation. ABLIM1, GAP43 and L1CAM all play crucial roles in RGC axon growth and pathfinding by mediating cytoskeleton changes or cell-cell interactions (Demmyanenko and Maness, 2003; Erkman et al., 2000; Suh et al., 2004; Zhang et al., 2000). SHH is secreted by differentiated RGCs and negatively regulates the differentiation of retinal progenitors into RGCs (Wang et al., 2005; Wang et al., 2002b; Zhang and Yang, 2001). When compared with the controls, the expression of the above genes in the GCL was reduced in mice lacking either *Isl1* or *Brn3b* (Fig. 5; see Table S1 in the supplementary material). Interestingly, we also observed that the reduction in the expression of *Brn3a*, *Olf1* and *Ablim1* was less severe in *Isl1* null than in *Brn3b* null retinas (Fig. 5A,C,E). By contrast, a more significant decrease in *Isl2* expression was seen in *Isl1*-null retinas (Fig. 5B). The expression analysis presented here not only supports a direct role of ISL1 in RGC differentiation but also suggests that ISL1 and BRN3B probably function cooperatively through regulating the common downstream target genes.

Isl1-null mutants are defective in RGC axon growth and pathfinding

As several *Isl1* downstream genes are involved in axon growth and/or pathfinding, we suspected that ISL1 might regulate axon behavior and that axon targeting defects might be the trigger of RGC apoptosis in *Isl1* nulls. We anterogradely traced RGC axons by placing DiI crystals at the optic nerve heads of fixed embryos. Consistent with the observation that the pioneer RGC axons reach the optic chiasm at E12.5 in mice (Marcus and Mason, 1995), our analysis revealed that in the wild-type embryos at E13.5, a large proportion of RGC axons already passed the midline of the optic chiasm and extended in the contralateral optic tract. At the same time, a sizeable proportion of axons turned away from the midline and proceeded in the ipsilateral optic tract (Fig. 6A). However, in *Isl1* nulls and *Brn3b* nulls (Fig. 6B,C), most axons failed to reach the midline at E13.5. At E15.5, the optic chiasm structure in wild-type mice was well defined and resembled its adult-like

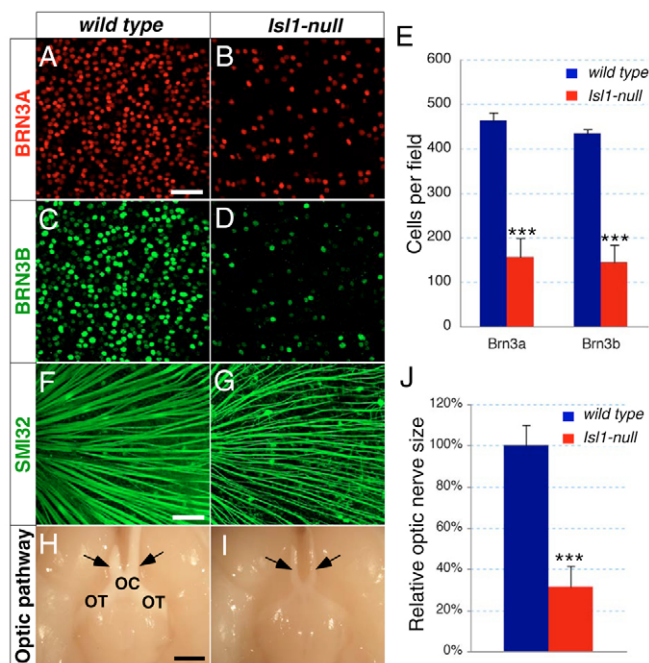


Fig. 4. Loss of RGCs in adult *Isl1*-null retina. (A-G) Immunostaining of whole-mount retina with anti-BRN3A (A,B), BRN3B (C,D), and SMI32 (F,G) antibodies reveals the reduction of RGCs in *Isl1*-null retina. (E) Quantification of BRN3A+ and BRN3B+ cells in the central retinal region of the whole mounts ($n=4$ for each genotype) reveals a loss of 66% RGCs in *Isl1*-null retina. (H,I) Ventral views of brain show the thinner optic nerves (arrows) in *Isl1* nulls. (J) Quantification of optic nerve size by measuring the cross area of H&E stained optic nerve transverse sections at the level indicated by arrows. Mean size of optic nerve in *Isl1*-null mice is reduced to 31% of that in wild type ($n=6$ pairs). Each histogram represents the mean+s.d. *** $P<0.001$ (t -test). OC, optic chiasm; OT, optic tract. Scale bars: 50 μ m in A; 100 μ m in F; 1 mm in H.

morphology (Fig. 6D). In both *Isl1* nulls and *Brn3b* nulls, though RGC axons projected into the contra- and ipsilateral optic tracts, several pathfinding defects were apparent (Fig. 6E,F). First, the optic nerves were smaller, indicating that a substantial fraction of RGCs failed to send out axons or that the axons did not exit the optic disc. Second, the axons in the optic tracts were less fasciculated and appeared to be grouped into two bundles (Fig. 6E,F, arrows). These observations are consistent with the recognized function of BRN3B in RGC axon growth and pathfinding (Erkman et al., 2000; Gan et al., 1999), and the similar roles of ISL1 in the projections of spinal motoneuron and sensory neuron axons (Kania and Jessell, 2003; Segawa et al., 2001; Thor and Thomas, 1997). Taken together, our data suggest that the axon growth defects occur prior to the onset of RGC apoptosis and may contribute to RGC death in both mutants.

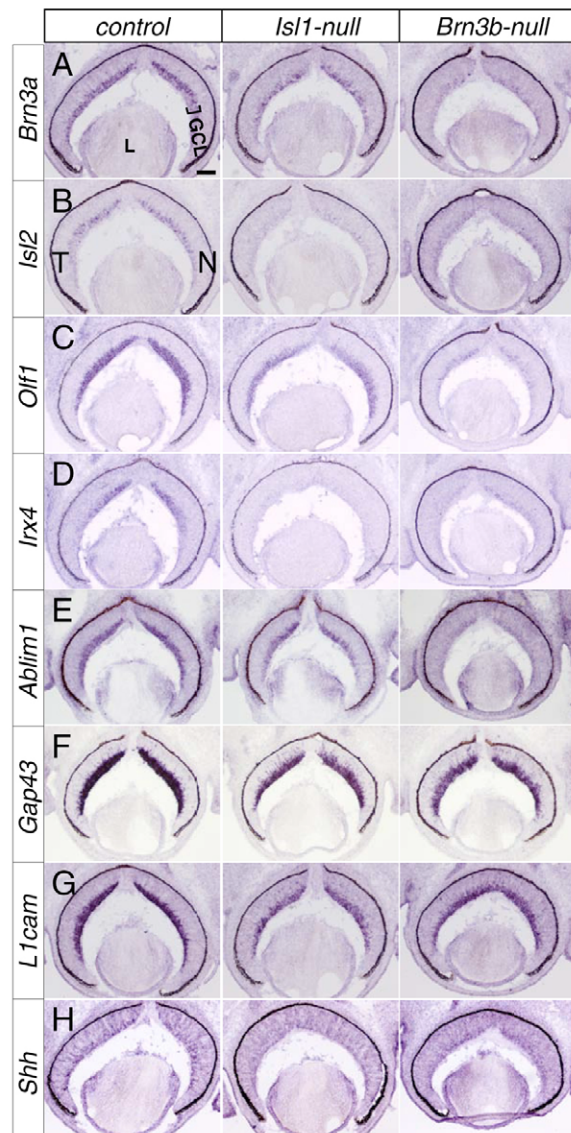


Fig. 5. ISL1 and BRN3B regulate the expression of a common set of RGC-specific genes. (A-H) Compared with controls (left panels), in situ hybridization shows that at E14.5, the expression of RGC-specific genes *Brn3a*, *Isl2*, *Olf1*, *Irx4*, *Ablim1*, *Gap43*, *L1cam* and *Shh* decreases in the GCL (bracket) of both *Isl1*-null (middle panels) and *Brn3b*-null retinas (right panels). T, temporal; N, nasal. Scale bar: 100 μ m.

More severe RGC loss in *Isl1* and *Brn3b* compound null mice

Based on their similar expression patterns and roles during RGC development, and the known cooperativity of these two types of TFs, we reasoned that BRN3B and ISL1 could function synergistically in RGCs and expected to observe more severe phenotypes in *Isl1* and *Brn3b* compound null (*Isl1/Brn3b* null) mutants. We therefore compared the number of BRN3A+ RGCs in whole-mount adult retinas of control, *Isl1* nulls, *Brn3b* nulls and *Isl1/Brn3b* nulls. We observed a reduction in the number of BRN3A+ cells in *Isl1*-null and *Brn3b*-null retinas compared with controls (Fig. 7A-C). Strikingly, only a very few BRN3A+ cells were identified in *Isl1/Brn3b*-null retinas (Fig. 7D). Similarly, compared with the high density of SMI32+ axon bundles in controls (Fig. 7E) or even the reduced axon bundles in *Isl1* null or *Brn3b* null (Fig. 7F,G) retinas, only a very limited number of SMI32+ axon bundles were detected in *Isl1/Brn3b* nulls (Fig. 7H). Consistent with the reduction of axon bundles in the retinas, the optic nerves of *Isl1/Brn3b* nulls were barely detectable and those of *Isl1* nulls and *Brn3b* nulls were reduced to about 31% and 20% of the controls, respectively (Fig. 7I-L, $n=3$ each genotype). The striking RGC loss in the compound mutants resembled that in *Math5*-null mice where only about 5% of RGCs are generated (Brown et al., 2001; Lin et al., 2004; Wang et al., 2001). However, unlike *Math5*-null mutation, loss of both *Isl1* and *Brn3b* did not affect the genesis of RGCs. X-Gal staining of E13.5 retina sections revealed the comparable number of *Brn3b-lacZ*-labeled nascent RGCs in the NBL and GCL of control, *Brn3b*-null and *Isl1/Brn3b*-null mice (Fig. 7M-O). Taken together, these data imply that *Isl1* and *Brn3b* function together downstream of *Math5* to control the terminal differentiation but not the genesis of almost all RGCs.

Simultaneous binding of ISL1 and BRN3B to RGC-specific promoters

To investigate whether the cooperative function of ISL1 and BRN3B during RGC development was mediated by their direct regulation of RGC-specific genes, we explored the co-occupancy of these two factors on RGC-specific promoters in vivo with ChIP assays. The BRN3-binding site, ATNA(A/T)T(T/A)AT (Gruber et al., 1997; Trieu et al., 2003), was found in many genes expressed in RGCs. We examined four of them, *Brn3b*, *Shh*, *Brn3a* and *Isl2*, to determine whether they are directly regulated by both ISL1 and

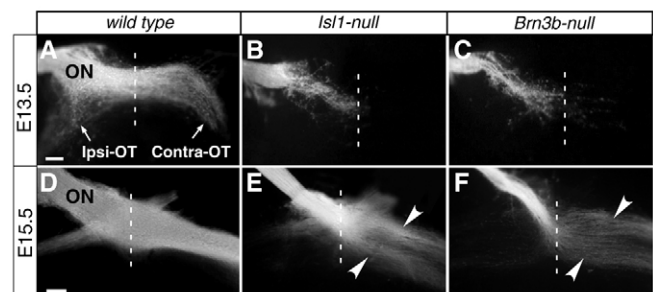


Fig. 6. Axon growth defects in mice deficient for *Isl1* or *Brn3b*. (A-F) Optic pathways at the ventral diencephalons after unilateral Dil labeling. In *Isl1* nulls and *Brn3b* nulls, the majority of RGC axons fails to reach the midline at E13.5 (A-C). At E15.5, although the chiasmata are formed in the null mice (D-F), the optic nerves are noticeably thinner and axons are de-fasciculated in the optic tract (arrowheads). ON, optic nerve; Ipsi-OT, ipsilateral optic tract; Contra-OT, contralateral optic tract. Scale bars: 100 μ m.

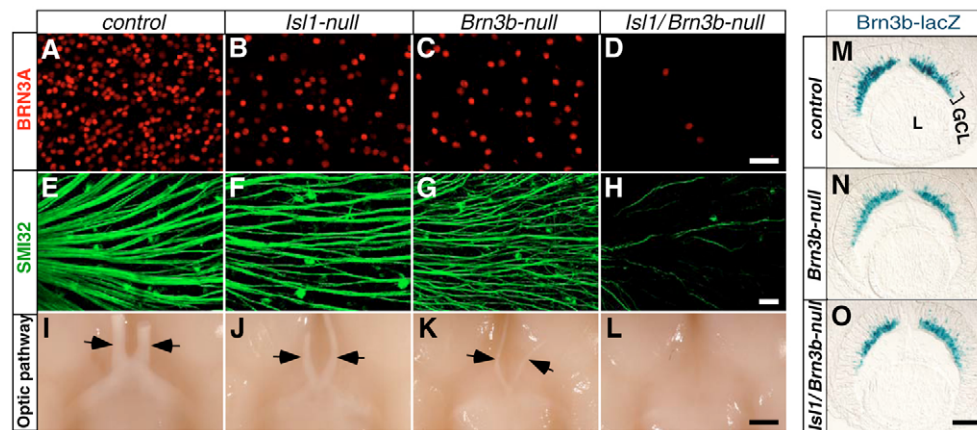


Fig. 7. More severe RGC loss in *Isl1* and *Brn3b* compound null mice. (A-H) Immunostaining of adult whole-mount retinas with anti-BRN3A (A-D) and SMI32 (E-H). A more severe loss of BRN3A+ RGCs (red) and SMI32+ axon bundles (green) is observed in *Isl1/Brn3b*-null retina. (I-L) Ventral views of brains reveal optic nerves (arrows). Compared with the controls (I), optic nerve size is reduced in *Isl1* nulls (J) and *Brn3b* nulls (K). The optic nerves are barely detectable in *Isl1/Brn3b*-null mice (L). (M-O) X-Gal staining of *Brn3b-lacZ*-expressing RGCs in E13.5 retina sections shows that the genesis and migration of RGCs are undisturbed in *Brn3b*-null (N) and *Isl1/Brn3b*-null (O) retinas. L, lens; GCL, ganglion cell layer. Scale bars: 50 μ m in D and H; 800 μ m in L and 100 μ m in O.

BRN3B. Besides *Brn3b*, these genes were chosen because their expression in RGCs immediately follows that of ISL1 and BRN3B (Quina et al., 2005; Wang et al., 2005; Xiang, 1998) and depends on ISL1 and BRN3B (Fig. 5). We immunoprecipitated the chromatin from wild-type retinas at E13.5-14.5 and PCR-amplified the promoter regions containing BRN3-binding consensus sequence. Both anti-ISL1 and anti-BRN3B antibodies co-precipitated with the promoter sequences of *Brn3b*, *Shh*, *Brn3a* and *Isl2* (Fig. 8A and Fig. S3 in the supplementary material). Neither of these antibodies precipitated with *Brn3b*-coding sequences in the controls (Fig. 8A). To further sustain the specificity of our assays, we also incorporate several negative controls, including IgG-precipitation, anti-BRN3B precipitation of chromatin derived from *Brn3b*-null retinas and anti-ISL1 precipitation with cerebellum tissues where ISL1 was not expressed. (Fig. 8A; see Fig. S3 in the supplementary material). Moreover, anti-ISL1 was not able to co-precipitate with these promoters in *Brn3b*-null retinas, implying that the binding of ISL1 to these promoters depends on BRN3B.

We further explored whether ISL1 and BRN3B synergistically regulate the expression of their targets using in vitro transactivation assay. We used the established *Brn3a*-luciferase transactivation assays in CV1 epithelial cells (Trieu et al., 2003) and co-transfected CV1 cells with *Brn3a*-luciferase reporter and *Isl1* and/or *Brn3b* expression plasmids. Although BRN3B alone activated *Brn3a*-luciferase expression to 2.34-fold of the control level (t -test $P < 0.001$) and ISL1 had no effect on *Brn3a*-luciferase expression (1.01-fold, $P > 0.05$), co-expression of ISL1 and BRN3B activated *Brn3a*-luciferase expression by 5.07 fold ($P < 0.001$, Fig. 8B). Thus, ISL1 and BRN3B simultaneously bind to and synergistically regulate the expression of their target genes.

DISCUSSION

TF networks have been shown to regulate the sequential events of neurogenesis including cell fate specification, differentiation and neuronal subtype determination (Castro et al., 2006; Lee and Pfaff, 2003; Shirasaki and Pfaff, 2002). Among these TFs, the POU-HD and LIM-HD TFs are often co-expressed in the same differentiating neurons and play essential roles during late stage of the neuronal

differentiation in both invertebrates and vertebrates. In this study, we use neural retina to explore the functional mechanism of LIM-HD and POU-HD TFs during neurogenesis. Using retina-specific knockout of *Isl1*, we show that similar to those in *Brn3b*-null retinas, a majority of RGCs in *Isl1*-nulls are defective in axon growth and pathfinding, and die prenatally. Moreover, a loss of greater than 95% RGCs in *Isl1/Brn3b* nulls, the necessity of both ISL1 and BRN3B for the expression of common downstream genes, and their simultaneous binding to and synergistic regulation of RGC-specific genes demonstrate the parallel and cooperative nature of ISL1 and BRN3B function in RGC development.

Expression and function of ISL1 in RGC development

The onset of ISL1 expression in post-mitotic cells at E11.5 and its complete co-localization with BRN3B in nascent RGCs suggest a role for ISL1 in RGC development. We found that targeted disruption of *Isl1* does not affect the genesis of RGCs. Rather, it results in the apoptosis of a significant number of RGCs (Fig. 3). The observed RGC defect in *Isl1*-null retinas is consistent with the spatiotemporal expression of ISL1 in nascent RGCs and supports its role in the late stages of RGC development. In addition to RGCs, ISL1 is also expressed in developing cholinergic amacrine and ON-bipolar cells in mouse retina (Elshatory et al., 2007a). In a separate study, we have examined the effect of the *Isl1*-null mutation on these other two types of retinal neurons and found the postnatal loss of nearly all these cells in the absence of *Isl1* (Elshatory et al., 2007b), further supporting its essential role in the late stages of retinal neurogenesis.

In normal retina development, about half of RGCs die during the first postnatal week owing to the deprivation of target-derived neurotrophins as the result of axon mis-projection (Farah and Easter, 2005; Perry et al., 1983). It is possible that the massive RGC death in *Isl1*-null or *Brn3b*-null retinas could also result from a similar mechanism, based on their recognized roles in axon guidance. In *Drosophila*, *Islet* is required for proper axon trajectory of spinal motoneurons (Thor and Thomas, 1997). Mis-expression of *Isl1* in chicken also causes axon targeting errors of the spinal motoneurons (Kania and Jessell, 2003). Moreover, mis-guidance of RGC axons

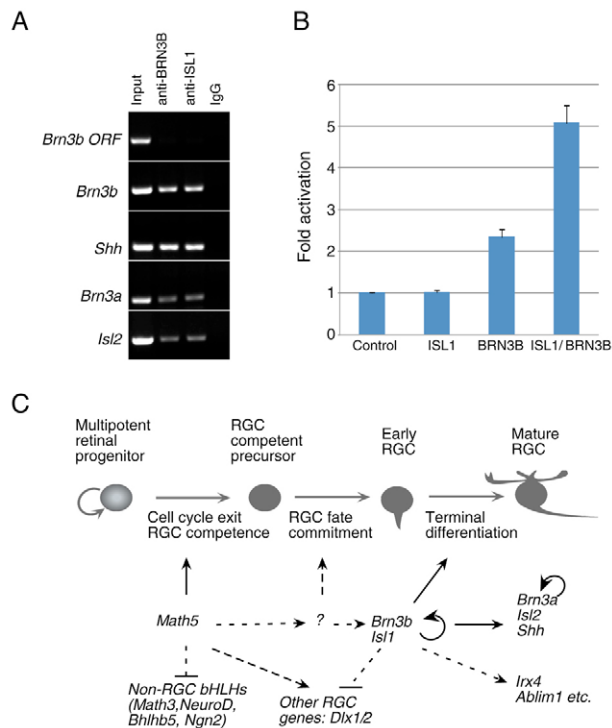


Fig. 8. Functional mechanism of ISL1 and BRN3B in the

development of RGCs. (A) Concurrent binding of ISL1 and BRN3B to RGC-specific promoters. Anti-BRN3B and anti-ISL1 antibodies but not IgG co-precipitate with the promoters of *Brn3b*, *Shh*, *Brn3a* and *Isl2*. Both antibodies do not precipitate with control *Brn3b* ORF.

(B) Functional synergy of ISL1 and BRN3B on *Brn3a* luciferase reporter gene expression. Cells transfected with empty pcDNA expression vector and reporter are used as controls. Luciferase activity is determined by normalizing firefly activity with renilla activity. Then fold activation is calculated by dividing the luciferase activity of experimental groups with that of control. Each histogram represents the mean±s.d. ($n=4$). **(C)** The Math5-Brn3b/Is11 pathway in the development of RGCs. Solid lines, direct regulation identified; broken lines, indirect or proposed regulation.

at multiple decision-making points has been reported in *Brn3b*-null mutants (Erkman et al., 2000). In this study, we show that the defect in RGC axons arises prior to RGC apoptosis in *Isl1* nulls or *Brn3b* nulls, suggesting that the defect in axon outgrowth and/or targeting contribute to the excessive apoptosis of RGCs. Interestingly, in *Isl1*-null or *Brn3b*-null retinas, there is a significant downregulation of genes implicated in axon growth (*Gap43*), fasciculation (*L1cam*) and guidance (*Isl2*, *Ablim1*) (Fig. 5). Furthermore, DiI anterograde tracing experiments reveal that at E13.5, a significant amount of pioneer RGC axons fail to reach the midline in *Isl1* nulls or *Brn3b* nulls (Fig. 6). At E15.5, although the optic chiasm does form in these null mutants, it is always associated with axon growth and fasciculation defects.

As loss of *Brn3b* results in a similar phenotype of RGC apoptosis, it is possible that ISL1 could regulate the terminal differentiation and survival of RGCs by maintaining *Brn3b* expression. Using anti-BRN3B immunostaining, we show that starting from E16.5, both the number of BRN3B+ RGCs and its expression intensity per cell decline in *Isl1*-null retinas (Fig. 3). ChIP assays show that both ISL1 and BRN3B bind to *Brn3b* promoter in vivo. Previously, it has been shown that after the initial expression, BRN3B maintains its own

expression by positive autofeedback regulation (Liu et al., 2001). Taken together, these data suggest that ISL1 and BRN3B co-bind to *Brn3b* promoter directly and maintain *Brn3b* expression in retina. The continuous expression of *Brn3b* then maintains the survival of developing RGCs.

Alternatively, ISL1 could directly control the terminal differentiation and survival of RGCs by regulating the expression of genes essential for these processes. Supporting this hypothesis are our findings that genes with expression in differentiating RGCs are significantly downregulated in *Isl1*-null retinas before the reduction of BRN3B expression and the initiation of RGC apoptosis (Fig. 5). Moreover, inconsistent with the reduced *Shh* expression and its role as a retinal progenitor mitogen, there is a slight decrease of M-phase retinal progenitors in *Isl1*-null retinas (see Fig. S4 in the supplementary material). The expression of these RGC genes is also diminished in *Brn3b* nulls, suggesting that these two TFs regulate a common set of downstream target genes. Interestingly, we have also noticed that the extent of downregulation of certain RGC genes differs in *Isl1* nulls than in *Brn3b* nulls. For example, the expression of *Brn3a*, *Olf1* and *Ablim1* is reduced more severely in *Brn3b* nulls, while *Isl2* expression is more significantly downregulated in *Isl1* nulls (Fig. 5), suggesting the expression of these genes could have different dependency on ISL1 than on BRN3B. BRN3B alone is probably sufficient to maintain the expression of *Brn3a*, *Olf1* and *Ablim1* in certain RGCs, whereas ISL1 is essential for the expression of *Isl2*. The resolution of this different dependency awaits the future transcriptional regulation analysis of these genes.

ISL1 and BRN3B co-regulate the RGC differentiation program

Our data indicate that ISL1 and BRN3B simultaneously bind to the promoter regions of RGC-specific genes and synergistically regulate their expression during RGC differentiation. This finding is consistent with prior studies of the cooperative function of POU-HD and LIM-HD factors. The POU-HD factor PIT1 (POU1F1 – Mouse Genome Informatics) and the LIM-HD factor P-LIM (LHX3 – Mouse Genome Informatics) are co-expressed during pituitary development. PIT1 and P-LIM interact with each other and both bind to promoter sequences containing PIT1-binding sites (Bach et al., 1995). The LIM-domains of P-LIM are not required for DNA binding but are crucial for the synergistic interaction with PIT1 on distal target genes, including *Pit1*. In *C. elegans*, UNC-86 dimerizes with MEC-3 to play an essential role in regulating the terminal differentiation of touch sensory cells (Duggan et al., 1998; Lichtsteiner and Tjian, 1995; Xue et al., 1992; Xue et al., 1993). However, in contrast to the interaction between PIT1 and P-LIM, the coupling of UNC-86 and MEC-3 does not require the LIM-domains and MEC-3 alone binds poorly to the promoters. In retina, we demonstrate that anti-ISL1 does not co-precipitate with promoters tested in the absence of BRN3B (see Fig. S3A in the supplementary material), suggesting the binding of ISL1 to these promoters depends on BRN3B. Moreover, ISL1 alone is not sufficient to activate *Brn3a*-luciferase reporter, but is essential for the synergetic activation of *Brn3a* when co-expressed with BRN3B (Fig. 8B).

Previous studies have shown by gel-shift assays that BRN3B binds to the BRN3-binding site (SBRN3) in the first intron of *Shh* and activates the expression of a reporter gene containing SBRN3 in cultured HEK293 cells (Mu et al., 2004). Using ChIP assay, we demonstrate that BRN3B binds to this SBRN3-containing region in vivo in the developing retinas. Additionally, we reveal the

simultaneously binding of ISL1 to the same region in the first intron of *Shh*. Intriguingly, ISL1 has also been reported as an upstream regulator of *Shh* during cardiac morphogenesis (Lin et al., 2006). It would be interesting to test whether ISL1 controls *Shh* expression through its first intron in developing heart.

Taken together, our expression and targeted deletion analysis suggests a *Math5-Is11/Brn3b* pathway of RGC development (Fig. 8C). The expression of MATH5 endows the post-mitotic precursors with RGC competence and activates the expression of *Is11* and *Brn3b* to initiate the RGC differentiation program. Math5 also suppresses the non-RGC differentiation pathways by negatively regulating the non-RGC specifying factors such as NGN2, NEUROD, MATH3 (NEUROG2, NEUROD1 and NEUROD4, respectively – Mouse Genome Informatics) and BHLHB5 (Feng et al., 2006; Mu et al., 2005a). As the loss of either *Is11* or *Brn3b* does not affect the initial expression of the other, their expression is regulated in parallel by upstream TFs such as MATH5. The joint action of ISL1 and BRN3B leads to the expression of RGC-specific genes including *Brn3a*, *Shh*, *Olf1* and *Ablim1*, as well as the autofeedback regulation of *Brn3b*. Although our data imply that the majority of RGCs require both factors to activate their terminal differentiation, the presence of a few RGCs in *Is11/Brn3b*-nulls suggests the existence of a pathway independent of BRN3B or ISL1. Published studies show that other TFs, such as DLX1 and DLX2, also participate in regulating the terminal differentiation and survival of 33% RGCs (de Melo et al., 2005). Interestingly, the expression of *Dlx1* and *Dlx2* is upregulated in *Brn3b*-null retinas, suggesting BRN3B normally represses *Dlx1/2* expression (Mu et al., 2004; Pan et al., 2005). Thus, it is possible that BRN3B and DLX1/2 are required for the development of complementary sets of RGCs (de Melo et al., 2005). Though the remaining RGCs in *Brn3b*-null retinas represent most or all RGC subtypes (Lin et al., 2004), it remains to be tested whether any specific RGC subtype is selectively lost in *Is11*-null or *Dlx1/2*-null mice.

In addition to retina, both ISL1 and BRN3 TFs are co-expressed in the developing dorsal root ganglia, trigeminal ganglia, and the spiral and vestibular ganglia of the inner ear (Artinger et al., 1998; Avivi and Goldstein, 1999; Huang et al., 2001; Radde-Gallwitz et al., 2004; Sohal et al., 1996). Our findings that BRN3B and ISL1 cooperate in RGC differentiation strongly argue for a common functional mechanism of these two classes of TFs in neurogenesis in these other areas of the developing nervous systems. It remains unknown whether these two factors directly couple with each other in transcriptional complexes. Interactions of LIM-HD proteins are generally mediated by LDB family co-factors with the direct interaction between UNC-86 and MEC-3 as the only exception (Hobert and Westphal, 2000; Lichtsteiner and Tjian, 1995). In combination with immunoprecipitation, future experiments, such as in vitro pull down, in vitro DNA binding and yeast two-hybrid assays, can be used to resolve the biochemistry nature of this interaction.

We thank Dr Alexandra Joyner for the W4 mouse ES cells, and Drs Amy Kiernan, Richard Libby, Eric Turner, Jason Lanier and the members of the Gan Laboratory for many helpful discussions and technical assistance. This work was supported by NIH grants (EY013426 and EY015551), Kilian and Caroline F. Schmitt Program on Integrative Brain Research to L.G., and the Research to Prevent Blindness challenge grant to Department of Ophthalmology at University of Rochester.

Supplementary material

Supplementary material for this article is available at <http://dev.biologists.org/cgi/content/full/135/11/1981/DC1>

References

- Appel, B., Korzh, V., Glasgow, E., Thor, S., Edlund, T., Dawid, I. B. and Eisen, J. S. (1995). Motoneuron fate specification revealed by patterned LIM homeobox gene expression in embryonic zebrafish. *Development* **121**, 4117–4125.
- Artinger, K. B., Fedtsova, N., Rhee, J. M., Bronner-Fraser, M. and Turner, E. (1998). Placodal origin of Brn-3-expressing cranial sensory neurons. *J. Neurobiol.* **36**, 572–585.
- Auerbach, W., Dunmore, J. H., Fairchild-Huntress, V., Fang, Q., Auerbach, A. B., Huszar, D. and Joyner, A. L. (2000). Establishment and chimera analysis of 129/SvEv- and C57BL/6-derived mouse embryonic stem cell lines. *Biotechniques* **29**, 1024–1028, 1030, 1032.
- Avivi, C. and Goldstein, R. S. (1999). Differential expression of Islet-1 in neural crest-derived ganglia: Islet-1 + dorsal root ganglion cells are post-mitotic and Islet-1 + sympathetic ganglion cells are still cycling. *Dev. Brain Res.* **115**, 89–92.
- Bach, I., Rhodes, S. J., Pearse, R. V., 2nd, Heinzel, T., Gloss, B., Scully, K. M., Sawchenko, P. E. and Rosenfeld, M. G. (1995). P-Lim, a LIM homeodomain factor, is expressed during pituitary organ and cell commitment and synergizes with Pit-1. *Proc. Natl. Acad. Sci. USA* **92**, 2720–2724.
- Bang, A. G. and Goulding, M. D. (1996). Regulation of vertebrate neural cell fate by transcription factors. *Curr. Opin. Neurobiol.* **6**, 25–32.
- Brown, A., Yates, P. A., Burrola, P., Ortuno, D., Vaidya, A., Jessell, T. M., Pfaff, S. L., O'Leary, D. D. and Lemke, G. (2000). Topographic mapping from the retina to the midbrain is controlled by relative but not absolute levels of EphA receptor signaling. *Cell* **102**, 77–88.
- Brown, N. L., Patel, S., Brzezinski, J. and Glaser, T. (2001). Math5 is required for retinal ganglion cell and optic nerve formation. *Development* **128**, 2497–2508.
- Castro, D. S., Skowronska-Krawczyk, D., Armant, O., Donaldson, I. J., Parras, C., Hunt, C., Critchley, J. A., Nguyen, L., Gossler, A., Gottgens, B. et al. (2006). Proneural bHLH and Brn proteins coregulate a neurogenic program through cooperative binding to a conserved DNA motif. *Dev. Cell* **11**, 831–844.
- Cepko, C. L., Austin, C. P., Yang, X., Alexiades, M. and Ezzeddine, D. (1996). Cell fate determination in the vertebrate retina. *Proc. Natl. Acad. Sci. USA* **93**, 589–595.
- de Melo, J., Du, G., Fonseca, M., Gillespie, L. A., Turk, W. J., Rubenstein, J. L. and Eisenstat, D. D. (2005). Dlx1 and Dlx2 function is necessary for terminal differentiation and survival of late-born retinal ganglion cells in the developing mouse retina. *Development* **132**, 311–322.
- Demyanenko, G. P. and Maness, P. F. (2003). The L1 cell adhesion molecule is essential for topographic mapping of retinal axons. *J. Neurosci.* **23**, 530–538.
- Duggan, A., Ma, C. and Chalfie, M. (1998). Regulation of touch receptor differentiation by the *Caenorhabditis elegans* mec-3 and unc-86 genes. *Development* **125**, 4107–4119.
- Elshatory, Y., Deng, M., Xie, X. and Gan, L. (2007a). Expression of the LIM-homeodomain protein Isl1 in the developing and mature mouse retina. *J. Comp. Neurol.* **503**, 182–197.
- Elshatory, Y., Everhart, D., Deng, M., Xie, X., Barlow, R. B. and Gan, L. (2007b). Islet-1 controls the differentiation of retinal bipolar and cholinergic amacrine cells. *J. Neurosci.* **27**, 12707–12720.
- Erkman, L., McEvilly, R. J., Luo, L., Ryan, A. K., Hooshmand, F., O'Connell, S. M., Keithley, E. M., Rapaport, D. H., Ryan, A. F. and Rosenfeld, M. G. (1996). Role of transcription factors Brn-3.1 and Brn-3.2 in auditory and visual system development. *Nature* **381**, 603–606.
- Erkman, L., Yates, P. A., McLaughlin, T., McEvilly, R. J., Whisenhunt, T., O'Connell, S. M., Krones, A. I., Kirby, M. A., Rapaport, D. H., Bermingham, J. R. et al. (2000). A POU domain transcription factor-dependent program regulates axon pathfinding in the vertebrate visual system. *Neuron* **28**, 779–792.
- Farah, M. H. and Easter, S. S., Jr (2005). Cell birth and death in the mouse retinal ganglion cell layer. *J. Comp. Neurol.* **489**, 120–134.
- Feng, L., Xie, X., Joshi, P. S., Yang, Z., Shibasaki, K., Chow, R. L. and Gan, L. (2006). Requirement for Bhlhb5 in the specification of amacrine and cone bipolar subtypes in mouse retina. *Development* **133**, 4815–4825.
- Furuta, Y., Lagutin, O., Hogan, B. L. and Oliver, G. C. (2000). Retina- and ventral forebrain-specific Cre recombinase activity in transgenic mice. *Genesis* **26**, 130–132.
- Galli-Resta, L., Resta, G., Tan, S. S. and Reese, B. E. (1997). Mosaics of islet-1-expressing amacrine cells assembled by short-range cellular interactions. *J. Neurosci.* **17**, 7831–7838.
- Gan, L., Xiang, M., Zhou, L., Wagner, D. S., Klein, W. H. and Nathans, J. (1996). POU domain factor Brn-3b is required for the development of a large set of retinal ganglion cells. *Proc. Natl. Acad. Sci. USA* **93**, 3920–3925.
- Gan, L., Wang, S. W., Huang, Z. and Klein, W. H. (1999). POU domain factor Brn-3b is essential for retinal ganglion cell differentiation and survival but not for initial cell fate specification. *Dev. Biol.* **210**, 469–480.
- Gruber, C. A., Rhee, J. M., Gleiberman, A. and Turner, E. E. (1997). POU domain factors of the Brn-3 class recognize functional DNA elements which are distinctive, symmetrical, and highly conserved in evolution. *Mol. Cell Biol.* **17**, 2391–2400.

- Hoebert, O. and Westphal, H. (2000). Functions of LIM-homeobox genes. *Trends Genet.* **16**, 75-83.
- Huang, E. J., Liu, W., Fritsch, B., Bianchi, L. M., Reichardt, L. F. and Xiang, M. (2001). Brn3a is a transcriptional regulator of soma size, target field innervation and axon pathfinding of inner ear sensory neurons. *Development* **128**, 2421-2432.
- Jensen, A. M. and Wallace, V. A. (1997). Expression of Sonic hedgehog and its putative role as a precursor cell mitogen in the developing mouse retina. *Development* **124**, 363-371.
- Jin, Z., Zhang, J., Klar, A., Chedotal, A., Rao, Y., Cepko, C. L. and Bao, Z. Z. (2003). Irx4-mediated regulation of Slit1 expression contributes to the definition of early axonal paths inside the retina. *Development* **130**, 1037-1048.
- Kania, A. and Jessell, T. M. (2003). Topographic motor projections in the limb imposed by LIM homeodomain protein regulation of ephrin-A:EphA interactions. *Neuron* **38**, 581-596.
- Kania, A., Johnson, R. L. and Jessell, T. M. (2000). Coordinate roles for LIM homeobox genes in directing the dorsoventral trajectory of motor axons in the vertebrate limb. *Cell* **102**, 161-173.
- Komiyama, T., Johnson, W. A., Luo, L. and Jefferis, G. S. (2003). From lineage to wiring specificity. POU domain transcription factors control precise connections of Drosophila olfactory projection neurons. *Cell* **112**, 157-167.
- Lee, S. K. and Pfaff, S. L. (2001). Transcriptional networks regulating neuronal identity in the developing spinal cord. *Nat. Neurosci. (Suppl.)* **4**, 1183-1191.
- Lee, S. K. and Pfaff, S. L. (2003). Synchronization of neurogenesis and motor neuron specification by direct coupling of bHLH and homeodomain transcription factors. *Neuron* **38**, 731-745.
- Lichtsteiner, S. and Tjian, R. (1995). Synergistic activation of transcription by UNC-86 and MEC-3 in *Caenorhabditis elegans* embryo extracts. *EMBO J.* **14**, 3937-3945.
- Lin, B., Wang, S. W. and Masland, R. H. (2004). Retinal ganglion cell type, size, and spacing can be specified independent of homotypic dendritic contacts. *Neuron* **43**, 475-485.
- Lin, L., Bu, L., Cai, C. L., Zhang, X. and Evans, S. (2006). Isl1 is upstream of sonic hedgehog in a pathway required for cardiac morphogenesis. *Dev. Biol.* **295**, 756-763.
- Liu, W., Mo, Z. and Xiang, M. (2001). The Ath5 proneural genes function upstream of Brn3 POU domain transcription factor genes to promote retinal ganglion cell development. *Proc. Natl. Acad. Sci. USA* **98**, 1649-1654.
- Marcus, R. C. and Mason, C. A. (1995). The first retinal axon growth in the mouse optic chiasm: axon patterning and the cellular environment. *J. Neurosci.* **15**, 6389-6402.
- Mu, X., Beremand, P. D., Zhao, S., Pershad, R., Sun, H., Scarpa, A., Liang, S., Thomas, T. L. and Klein, W. H. (2004). Discrete gene sets depend on POU domain transcription factor Brn3b/Brn-3.2/POU4f2 for their expression in the mouse embryonic retina. *Development* **131**, 1197-1210.
- Mu, X., Fu, X., Sun, H., Beremand, P. D., Thomas, T. L. and Klein, W. H. (2005a). A gene network downstream of transcription factor Math5 regulates retinal progenitor cell competence and ganglion cell fate. *Dev. Biol.* **280**, 467-481.
- Mu, X., Fu, X., Sun, H., Liang, S., Maeda, H., Frishman, L. J. and Klein, W. H. (2005b). Ganglion cells are required for normal progenitor- cell proliferation but not cell-fate determination or patterning in the developing mouse retina. *Curr. Biol.* **15**, 525-530.
- Nixon, R. A., Lewis, S. E., Dahl, D., Marotta, C. A. and Drager, U. C. (1989). Early posttranslational modifications of the three neurofilament subunits in mouse retinal ganglion cells: neuronal sites and time course in relation to subunit polymerization and axonal transport. *Mol. Brain. Res.* **5**, 93-108.
- Pak, W., Hindges, R., Lim, Y. S., Pfaff, S. L. and O'Leary, D. D. (2004). Magnitude of binocular vision controlled by islet-2 repression of a genetic program that specifies laterality of retinal axon pathfinding. *Cell* **119**, 567-578.
- Pan, L., Yang, Z., Feng, L. and Gan, L. (2005). Functional equivalence of Brn3 POU-domain transcription factors in mouse retinal neurogenesis. *Development* **132**, 703-712.
- Perry, V. H., Henderson, Z. and Linden, R. (1983). Postnatal changes in retinal ganglion cell and optic axon populations in the pigmented rat. *J. Comp. Neurol.* **219**, 356-368.
- Pfaff, S. L., Mendelsohn, M., Stewart, C. L., Edlund, T. and Jessell, T. M. (1996). Requirement for LIM homeobox gene Isl1 in motor neuron generation reveals a motor neuron-dependent step in interneuron differentiation. *Cell* **84**, 309-320.
- Quina, L. A., Pak, W., Lanier, J., Banwait, P., Gratwick, K., Liu, Y., Velasquez, T., O'Leary, D. D., Goulding, M. and Turner, E. E. (2005). Brn3a-expressing retinal ganglion cells project specifically to thalamocortical and collicular visual pathways. *J. Neurosci.* **25**, 11595-11604.
- Radde-Gallwitz, K., Pan, L., Gan, L., Lin, X., Segil, N. and Chen, P. (2004). Expression of Islet1 marks the sensory and neuronal lineages in the mammalian inner ear. *J. Comp. Neurol.* **477**, 412-421.
- Segawa, H., Miyashita, T., Hirate, Y., Higashijima, S., Chino, N., Uyemura, K., Kikuchi, Y. and Okamoto, H. (2001). Functional repression of Islet-2 by disruption of complex with Ldb impairs peripheral axonal outgrowth in embryonic zebrafish. *Neuron* **30**, 423-436.
- Sharma, K., Sheng, H. Z., Lettieri, K., Li, H., Karavanov, A., Potter, S., Westphal, H. and Pfaff, S. L. (1998). LIM homeodomain factors Lhx3 and Lhx4 assign subtype identities for motor neurons. *Cell* **95**, 817-828.
- Sharma, K., Leonard, A. E., Lettieri, K. and Pfaff, S. L. (2000). Genetic and epigenetic mechanisms contribute to motor neuron pathfinding. *Nature* **406**, 515-519.
- Shirasaki, R. and Pfaff, S. L. (2002). Transcriptional codes and the control of neuronal identity. *Annu. Rev. Neurosci.* **25**, 251-281.
- Sohal, G. S., Bockman, D. E., Ali, M. M. and Tsai, N. T. (1996). Dil labeling and homeobox gene islet-1 expression reveal the contribution of ventral neural tube cells to the formation of the avian trigeminal ganglion. *Int. J. Dev. Neurosci.* **14**, 419-427.
- Suh, L. H., Oster, S. F., Soehrmann, S. S., Grenningloh, G. and Sretavan, D. W. (2004). L1/Laminin modulation of growth cone response to EphB triggers growth pauses and regulates the microtubule destabilizing protein SCG10. *J. Neurosci.* **24**, 1976-1986.
- Tanabe, Y., William, C. and Jessell, T. M. (1998). Specification of motor neuron identity by the MNR2 homeodomain protein. *Cell* **95**, 67-80.
- Thor, S. and Thomas, J. B. (1997). The Drosophila islet gene governs axon pathfinding and neurotransmitter identity. *Neuron* **18**, 397-409.
- Trieu, M., Ma, A., Eng, S. R., Fedtsova, N. and Turner, E. E. (2003). Direct autoregulation and gene dosage compensation by POU-domain transcription factor Brn3a. *Development* **130**, 111-121.
- Tsichida, T., Ensini, M., Morton, S. B., Baldassare, M., Edlund, T., Jessell, T. M. and Pfaff, S. L. (1994). Topographic organization of embryonic motor neurons defined by expression of LIM homeobox genes. *Cell* **79**, 957-970.
- Wang, S. W., Kim, B. S., Ding, K., Wang, H., Sun, D., Johnson, R. L., Klein, W. H. and Gan, L. (2001). Requirement for math5 in the development of retinal ganglion cells. *Genes Dev.* **15**, 24-29.
- Wang, S. W., Mu, X., Bowers, W. J., Kim, D. S., Plas, D. J., Crair, M. C., Federoff, H. J., Gan, L. and Klein, W. H. (2002a). Brn3b/Brn3c double knockout mice reveal an unsuspected role for Brn3c in retinal ganglion cell axon outgrowth. *Development* **129**, 467-477.
- Wang, Y. P., Dakubo, G., Howley, P., Campsall, K. D., Mazarolle, C. J., Shiga, S. A., Lewis, P. M., McMahon, A. P. and Wallace, V. A. (2002b). Development of normal retinal organization depends on Sonic hedgehog signaling from ganglion cells. *Nat. Neurosci.* **5**, 831-832.
- Wang, Y., Dakubo, G. D., Thurig, S., Mazarolle, C. J. and Wallace, V. A. (2005). Retinal ganglion cell-derived sonic hedgehog locally controls proliferation and the timing of RGC development in the embryonic mouse retina. *Development* **132**, 5103-5113.
- Xiang, M. (1998). Requirement for Brn-3b in early differentiation of postmitotic retinal ganglion cell precursors. *Dev. Biol.* **197**, 155-169.
- Xiang, M., Zhou, L., Macke, J. P., Yoshioka, T., Hendry, S. H., Eddy, R. L., Shows, T. B. and Nathans, J. (1995). The Brn-3 family of POU-domain factors: primary structure, binding specificity, and expression in subsets of retinal ganglion cells and somatosensory neurons. *J. Neurosci.* **15**, 4762-4785.
- Xue, D., Finney, M., Ruvkun, G. and Chalfie, M. (1992). Regulation of the mec-3 gene by the *C. elegans* homeoproteins UNC-86 and MEC-3. *EMBO J.* **11**, 4969-4979.
- Xue, D., Tu, Y. and Chalfie, M. (1993). Cooperative interactions between the *Caenorhabditis elegans* homeoproteins UNC-86 and MEC-3. *Science* **261**, 1324-1328.
- Yang, Z., Ding, K., Pan, L., Deng, M. and Gan, L. (2003). Math5 determines the competence state of retinal ganglion cell progenitors. *Dev. Biol.* **264**, 240-254.
- Young, R. W. (1985). Cell differentiation in the retina of the mouse. *Anat. Rec.* **212**, 199-205.
- Zhang, X. M. and Yang, X. J. (2001). Regulation of retinal ganglion cell production by Sonic hedgehog. *Development* **128**, 943-957.
- Zhang, F., Lu, C., Severin, C. and Sretavan, D. W. (2000). GAP-43 mediates retinal axon interaction with lateral diencephalon cells during optic tract formation. *Development* **127**, 969-980.